AD-A069 500   PRINCETON UNIV N J DEPT OF CHEMICAL ENGINEERING   F/G 7/3
              PYROLYSIS-MOLECULAR WEIGHT CHROMATOGRAPHY-VAPOR PHASE INFRARED --ETC(U)
              MAY 79 E KIRAN, J K GILLHAM   N00014-76-C-0200
UNCLASSIFIED   TR-16   NL

| OF |
AD
A069500

END
DATE
FILMED
7--79
DDC

Pyrolysis-Molecular Weight Chromatography-Vapor

Phase Infrared Spectrophotometry: An On-Line

System for Analysis of Polymers

by

E. Kiran and J. K. Gillham

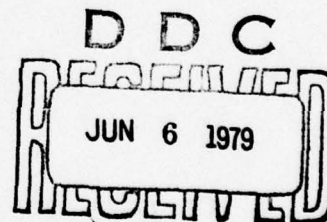Prepared for Publication as a Chapter in

"Developments in Polymer Degradation-2"

Editor: Professor N. Grassie

Applied Science Publishers Ltd., London, England

Polymer Materials Program
Department of Chemical Engineering
Princeton University
Princeton, NJ 08544

May 1979

JUN 6 1979

J. K. Gillham
Principal Investigator
609/452-4694

79 06 04 103

PYROLYSIS-MOLECULAR WEIGHT CHROMATOGRAPHY-VAPOR PHASE

INFRARED SPECTROPHOTOMETRY: AN ON-LINE SYSTEM

FOR ANALYSIS OF POLYMERS

Erdoğan Kiran
SEKA (Türkiye Selüloz ve Kağit Fabrikalari Isletmesi)
Central Research Laboratory
Izmit, Kocaeli, Turkey

and

John K. Gillham
Polymer Materials Program
Department of Chemical Engineering
Princeton University
Princeton, New Jersey 08540   USA

An instrumental system consisting of a combination of a program-
mable pyrolyzer, a thermal conductivity detector, a mass chromatograph,
a gas chromatograph, a fast-scan vapor-phase infrared spectrophotometer
and a computer is discussed and reviewed with examples which show the
utility of the system in the analysis of decomposition phenomena in poly-
olefins, polyolefinsulfones, polymethacrylates, polystyrenes, and poly-
butadienes.

The system records the thermal history before and during pyrolysis
of the sample and provides chromatographic retention times, infrared
spectra, mass numbers and relative amounts of the volatile products of
pyrolysis. Identification of the constituents of the effluents is thus
facilitated and mechanisms for decomposition become easier to propose and
to verify.

INTRODUCTION

Pyrolytic decomposition followed by analysis of the volatile products of pyrolysis is a powerful method for characterization of polymeric materials. The scope and applicability of this approach are determined by the type of pyrolyzer and the separation and identification techniques that are utilized.

The on-line system developed at Princeton University comprises a programmable pyrolyzer, a thermal conductivity cell, a trap, a mass chromatograph, a conventional gas chromatograph, a vapor-phase infrared spectrophotometer, and a digital computer (1,2,3). The system has proved powerful for analysis of polymers as has been shown by results obtained with polyolefins (1,4,5,6,7), polyolefinsulfones (1,8), polymethacrylates (1), polystyrenes (1,3,8,9) and polybutadienes (10). This report provides a brief description of the system and reviews results obtained with these polymers.

THE PYROLYSIS LABORATORY

A schematic diagram of the system is shown in Figure 1. A critical discussion of its various parts has been presented elsewhere (2). Briefly, the system consists of a programmable pyrolyzer, a thermal conductivity cell (TC), a trap, a mass chromatograph (MC), a conventional gas chromatograph (GC), a vapor-phase infrared spectrophotometer (Vapor Phase IR) and a digital computer (IBM System 7).

Figure 2 shows details of the coupling of the pyrolyzer with the thermal conductivity detector, the trap, and the mass chromatograph.

The pyrolyzer consists of a quartz tube and an external heater which provides flexibility for either program-heating or flash-heating.

The thermal conductivity cell monitors the formation of the volatile products of pyrolysis as a function of temperature and time. It provides immediate information about the onset and the progress of the thermal events that result in the formation of volatile products. The response curves contain features that are characteristic of the material under investigation.

The combination of the pyrolyzer with the thermal conductivity detector is complementary to a thermogravimetric analyzer and/or differential thermal analyzer. As an example, the thermal history before and during pyrolysis of poly(pentene-1-sulfone) as recorded with the thermal conductivity cell (TC), a thermogravimetric analyzer (TGA) and a differential thermal analyzer (DTA) is shown in Figure 3.

The trap is an important part of the interface between the pyrolysis assembly and the chromatographic assembly. It is a short stainless steel column packed with Porapak Q (Waters Associates) and has a geometry which permits a fraction of it to be placed in a Dewar flask for subambient cooling. The function of the trap is to collect the fragments of pyrolysis that are formed in the temperature range of interest (i.e. selective trapping). The products are released from the trap by rapid heating, and introduced as a slug to the chromatographic columns for separation. The valving system permits monitoring of the release of the products from the trap with the same thermal conductivity cell used to monitor the formation of volatile products; the response is recorded as a sharp peak, as shown for example in Figure 4.

The mass chromatograph is a special type of a gas chromatograph which directly provides mass numbers of the resolved components of a mixture by

means of a pair of gas density detectors (11). The instrument consists of two independent gas chromatographs which use a common injection port. When a sample is introduced to the instrument it is split into two approximately equal fractions (splitter, Figure 2) and each fraction is carried to a trap which is similar to the trap associated with the pyrolyzer. Then, through a valve arrangement, different carrier gases are introduced to the two traps; the samples, released by rapid heating of the traps, are carried over to two matched chromatographic columns for separation. The constituents eluting from the chromatographic columns are detected by gas density detectors. The recorder output from the mass chromatograph displays two sets of peaks corresponding to the responses from the two gas chromatographic systems with different carrier gases for the same constituents of the mixture (see Figures 3 and 4).

Theoretical aspects and operational principles of the mass chromatograph and the gas density detector are presented elsewhere (1,11). The ratio of the responses is related to the molecular weight (M_x) of a constituent through

$$M_x = \frac{\left(\frac{A_1}{A_2}\right) K \, M_{C_2} - M_{C_1}}{\left(\frac{A_1}{A_2}\right) K - 1}$$

where M_{C_1} and M_{C_2} are the molecular weights of the carrier gases 1 and 2, A_1 and A_2 are the chromatographic peak areas for the constituent, and K is the instrument constant determined from analysis of samples of known molecular weights from

$$K = \left(\frac{M_x - M_{C_1}}{M_x - M_{C_2}}\right) \bigg/ \left(\frac{A_1}{A_2}\right).$$

The response of the gas density detector is proportional to $(M_x - M_C)/M_x$ and therefore, for a given carrier gas of molecular weight M_C, the response tends to a constant as M_x increases; the lower the molecular weight of the carrier gas, the faster is this tendency. In order to cover a wide range of molecular weights, the two carrier gases are chosen to be of highly different molecular weights. The gases used in these studies were CO_2 and ClC_2F_5 (Freon-115). Use of CO_2 and SF_6 is reported (12) in a study of oxidative degradation of isotactic poly(1-pentene) using a combination of a thermal conductivity detector and a mass chromatograph.

Since the molecular weights of the carrier gases are known and since the response ratios (A_1/A_2) can be measured from the chromatographic output, calculation of the molecular weights of the constituents becomes a simple process after the instrument constant is evaluated. In principle, the instrument constant K can be evaluated by injecting just one solute (of known molecular weight) into the mass chromatograph and measuring the response ratio from the output. However, the accuracy of measuring the response ratio varies with molecular weight and consequently K must be evaluated by using more than one compound if it is to be applicable to a wide range of molecular weights. Otherwise instantaneous K values applicable in small ranges are used.

In addition to providing mass numbers of resolved constituents the mass chromatograph can be used to provide estimates of the weight amounts of each (w_i). This is performed by comparing the areas on the CO_2 channel output of the mass chromatograph with those of peaks obtained under the same chromatographic conditions from a synthetic mixture containing known amounts of n-hydrocarbons (3). For compounds of very similar molecular

weight and with a similar retention time, responses of the gas density balance detector are directly proportional to their amounts (see equation 71 of reference 11). The relative amount of a component as a weight percentage (P_{wt}) of those measured can be calculated using $P_{wt} = (w_i / \Sigma w_i) \times 100$.

The infrared spectrophotometer is a fast-scan vapor-phase infrared spectrophotometer and is suitable for taking "on-the-fly" spectra of constituents eluting from chromatographic columns. The instrument is capable of scanning from 2.5 to 15 μm (4000 to 670 cm^{-1}) in either 6 or 30 seconds. The spectrophotometer can be coupled with either the mass chromatograph or the conventional gas chromatograph. When coupled with the mass chromatograph sensitivity is reduced due to the fact that column effluents are highly diluted by the reference gas entering the gas density detector. Furthermore the IR spectra of the carrier gases, CO_2 and Freon-115, are complex and can mask spectra of constituents (2). Therefore coupling of infrared spectrophotometer with a conventional gas chromatograph is preferred. A schematic of the coupling of the gas chromatograph with the infrared spectrophotometer and the computer is shown in Figure 5.

The gas chromatograph used is a computer-compatible, automated research instrument equipped with thermal conductivity and flame ionization detectors.

The computer facility is a flexible mini-computer capable of preprocessing of data for analysis by a much larger computational system (to which it is connected by telephone). As a constitutent elutes from the chromatographic column it may be trapped in the IR cell and a set number of IR spectra taken. These spectra are computer-averaged and the background spectrum is subtracted in order to increase the signal-to-noise ratio.

THERMAL DECOMPOSITION OF POLYMERS

Thermal decomposition of various polymers has been studied by the on-line system just described. Polymers studied include: 1) polyolefins (1,4,5,6,7); 2) polyolefinsulfones (1,8); 3) polymethacrylates (1); 4) polystyrenes (1,3,8,9) and 5) polybutadienes (10). Comparative discussions with literature reports on the same polymers using different techniques have been presented in references 1 to 11.
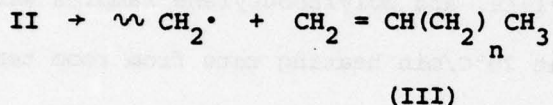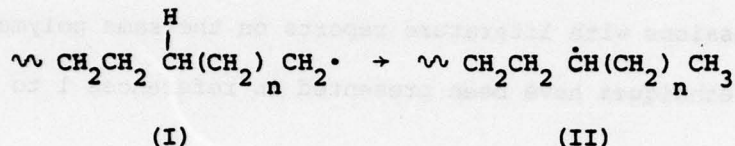
1) Polyolefins

Polyethylene, polypropylene, and polyisobutylene samples were pyrolyzed in flowing helium at 20°C/min heating rate from room temperature to 600°C. Products volatilizing in the temperature range 300-600°C were selected for trapping and analysis.

The output from the mass chromatograph for low density polyethylene is shown in Figure 6. The regularly spaced doublet peaks were shown to correspond to alkenes and alkanes by calculating the molecular weights and comparing the retention times with hydrocarbons (1,7). Molecular weights calculated from the mass chromatographic output for some of the assigned structures are given in Table I. The formation of the hydrocarbon constituents seen in Figure 6 and the observed relative abundance of C_6, C_{10}, C_{14} and C_{18} alkenes and C_3, C_7, C_{11} and C_{15} alkanes were considered to follow from an intramolecular radical transfer process which involves the 5th carbon atom of the primary macroradical through a pseudo six-membered ring intermediate. The presence of ethylene is not seen in Figure 6 since the column conditions were not suitable for its analysis.

Main chain scission in polyethylene results initially in primary radicals which can undergo either depolymerization or intra and/or intermolecular radical transfer processes. The relative extents of the

competing reactions determines the degradation pattern.

Intramolecular radical transfer reactions in primary radicals (I) lead to the formation of secondary radicals (II). These can undergo β-scission to the left of the radical center and produce alkenes (III).

$$\sim CH_2CH_2 \overset{\overset{\displaystyle H}{|}}{CH}(CH_2)_n CH_2\cdot \rightarrow \sim CH_2CH_2 \overset{\cdot}{CH}(CH_2)_n CH_3$$

(I)   (II)

$$II \rightarrow \sim CH_2\cdot + CH_2 = CH(CH_2)_n CH_3$$

(III)

If the β-scission is to the right of the radical center short chain primary radicals (IV) form

$$II \rightarrow \sim CH_2CH_2CH = CH_2 + \cdot CH_2(CH_2)_{n-2} CH_3$$

(IV)
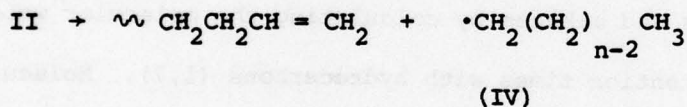
which can abstract a hydrogen atom from another molecule and produce alkanes (V).

$$CH_3(CH_2)_{n-2} CH_3$$

(V)
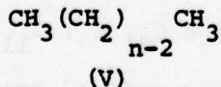
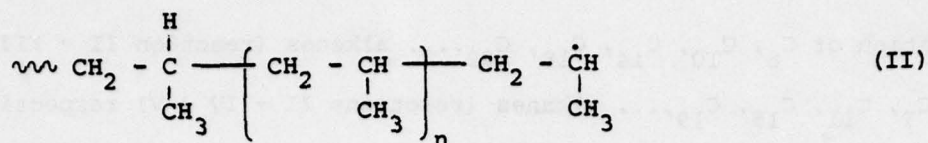Highly strained conformations will not be permitted in the intramolecular backbiting steps. The process is therefore argued to involve preferentially the fifth carbon atom through a pseudo six-membered ring intermediate. If subsequent repetitive intramolecular transfer follows before chain scission, the consequence of preferential radical transfer to the 5th, 9th, 13th, 17th, and 21st,...... carbon atoms is the preferential

formation of C_6, C_{10}, C_{14}, C_{18}, C_{22},... alkenes (reaction II → III) and C_3, C_7, C_{11}, C_{15}, C_{19},... alkanes (reactions II → IV → V) respectively. The probability of sequential migration of the free radical along the chain without undergoing β-scission reactions is expected to decrease as the number of transfer steps increases. One and two step processes should be most dominant and, as observed in Figure 6, among alkenes C_6 and C_{10}, and among alkanes C_3 and C_7 represent major constituents.
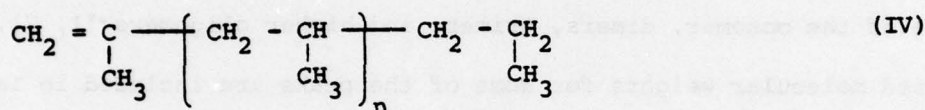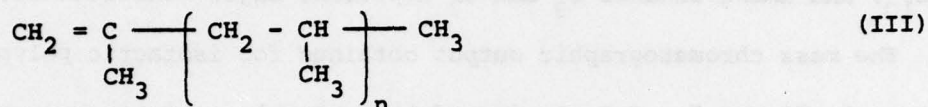
The mass chromatographic output obtained for isotactic polypropylene is shown in Figure 7. Calculation of the molecular weights has shown that the peaks in the chromatogram have molecular weights corresponding to those of the monomer, dimers, trimers and higher oligomers (1, 7). Calculated molecular weights for some of the peaks are included in Table I. The monomer (peak 1), which is formed extensively, is produced from either the primary or the secondary radicals formed on chain homolysis. Intramolecular radical transfers to the 6th, 10th, and 12th carbon atoms in the primary macroradicals and to the 5th and 9th and also the 13th carbon atoms in the secondary macroradicals (indexing from the secondary carbon radical at the chain end) account for the other major products of decomposition. The formation of the other volatile products of pyrolysis of polypropylene and their relative abundances have been explained also in terms of intramolecular radical transfer processes. In polypropylene initiation by chain scission results in primary (I) and secondary (II) radicals.

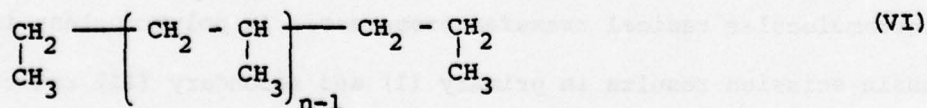$$\text{\Large$\wedge\wedge\wedge$ } CH_2 - \overset{\overset{\displaystyle H}{|}}{\underset{\underset{\displaystyle CH_3}{|}}{C}} \overbrace{\left(CH_2 - \overset{}{\underset{\underset{\displaystyle CH_3}{|}}{CH}} \right)}_{n} \dot{C}H_2 \qquad (I)$$

$$\text{\textasciitilde\textasciitilde\textasciitilde} CH_2 - \underset{\underset{CH_3}{|}}{\overset{\overset{H}{|}}{C}} \left(CH_2 - \underset{\underset{CH_3}{|}}{CH} \right)_n CH_2 - \overset{\bullet}{\underset{\underset{CH_3}{|}}{CH}} \tag{II}$$
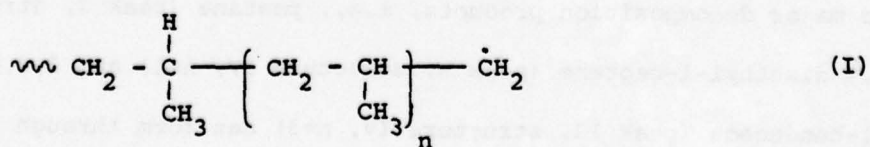
Intramolecular transfer reactions followed by β-scission to the left of
the resulting tertiary radical produces alkenes (III) from primary radi-
cals and alkenes (IV) from secondary radicals.

$$CH_2 = \underset{\underset{CH_3}{|}}{C} \left(CH_2 - \underset{\underset{CH_3}{|}}{CH} \right)_n CH_3 \tag{III}$$

$$CH_2 = \underset{\underset{CH_3}{|}}{C} \left(CH_2 - \underset{\underset{CH_3}{|}}{CH} \right)_n CH_2 - \underset{\underset{CH_3}{|}}{CH_2} \tag{IV}$$

β-scission to the right of the tertiary radical, followed by hydrogen

atom abstraction, leads to the formation of alkanes (V) and (VI) from

primary and secondary macroradicals, respectively.

$$\underset{\underset{CH_3}{|}}{CH_2} \left(CH_2 - \underset{\underset{CH_3}{|}}{CH} \right)_{n-1} CH_3 \tag{V}$$

$$\underset{\underset{CH_3}{|}}{CH_2} \left(CH_2 - \underset{\underset{CH_3}{|}}{CH} \right)_{n-1} CH_2 - \underset{\underset{CH_3}{|}}{CH_2} \tag{VI}$$

Specific major decomposition products, i.e., pentane (peak 3, structure VI,

n=1), 2,4 dimethyl-1-heptene (peak 9, structure IV, n=1) and 2,4,6,8 tetra-

methyl-1-hendecene (peak 12, structure IV, n=3) can form through intra-

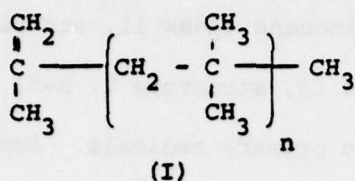molecular radical transfer in the secondary radicals, and 2-methylpentane

(peak 5, structure V, n=2), 2,4,6-trimethylnonane (peak 11, structure V, n=4) and 2,4,6,8-tetramethylhendecane (peak 13, structure V, r=5) can form from intramolecular radical transfer in the primary radicals. Among the higher molecular weight fragments 2,4,6,8,10,12 hexamethyl-1-tridecene (peak 16) and 2,4,6,8,10,12 hexamethyl-1-pentadecene (peak 17) are formed in larger amounts. Their formation is a continuation of the processes leading to peaks 12 and 13 which are major decomposition products.

The mass chromatogram for polyisobutylene displays a series of regularly spaced groups of peaks which is characteristic of a homologous series of products (Figure 8). In addition to depolymerization processes which account for the extensive formation of the monomer (peak 1), intramolecular radical transfer processes in the primary and tertiary macroradicals which form on initial chain scission account for the formation of dimers, trimers, and high oligomers (1,7). More intramolecular transfer occurs in the primary radicals than the tertiary radicals for energetic reasons. A major product, the trimer 2,4,4,6,6-pentamethyl-1-heptene (peak 12), is formed from a primary radical via intramolecular radical transfer to a methyl group:
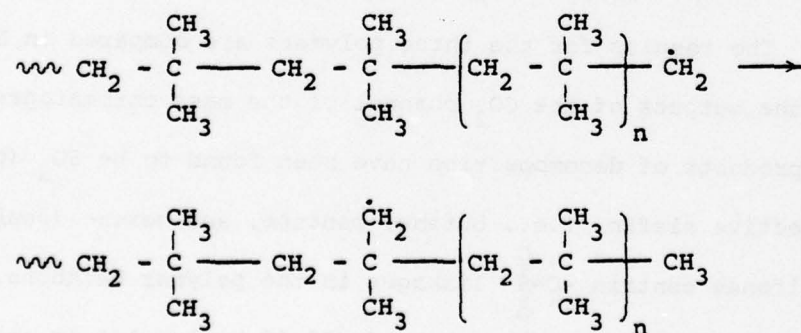
When the radical thus formed undergoes β-scission to the left of the adjacent carbon, alkenes with the structure (I) are formed:

$$
\begin{array}{c}
\overset{\displaystyle CH_2}{\underset{\displaystyle CH_3}{\overset{|}{\underset{|}{C}}}} \text{---} \left(CH_2 \text{---} \overset{\displaystyle CH_3}{\underset{\displaystyle CH_3}{\overset{|}{\underset{|}{C}}}} \right)_n \text{---} CH_3
\end{array}
$$

(I)

For n = 2 the alkene is the trimer 2,4,4,6,6-pentamethyl-1-heptene. In each quartet (peaks 14-29) the first two peaks correspond to alkenes which arise from tertiary radicals, but the last two, which are formed in larger amounts, to alkenes which are formed from primary radicals. For example in structure (I) n = 4 corresponds to peak 20, n = 5 to peak 24. Peaks 21 and 25 arise from primary radicals but via intramolecular radical transfer to methylene instead of a methyl group. Assigned structures and calculated molecular weights for some of the peaks are given in Table 1.

2) Polyolefinsulfones

Polybutene-1-sulfone, polypentene-1-sulfone and polyhexene-1-sulfone have been studied by pyrolyzing samples in helium at a heating rate of 20°C/min (1,8). The volatile products formed in the temperature range 100-500°C were analyzed by the mass chromatograph.

The mass chromatographic outputs are shown for polypentene-1-sulfone in Figure 3. The results for the three polymers are compared in Figure 9 in terms of the outputs of the CO_2 channel of the mass chromatograph. The primary products of decomposition have been found to be SO_2 (peak 1) and the respective olefin, i.e., butene, pentene, and hexene (peaks 2). These polysulfones contain $-\overset{\displaystyle O}{\underset{\displaystyle O}{\overset{||}{\underset{||}{\underset{|}{C}\text{-}\underset{|}{S}}}}}-$ linkages in the polymer backbone. The bond dissociation energy for the C-S bond (55-60 kcal/mole) is appreciably lower than for the C-C bond (80-85 kcal/mole) and the C-H bond (90-100 kcal/mole) (13). Consequently thermal decomposition in these polymers

may occur readily by scission of the C-S bond and results in the formation of SO_2 and the respective olefin.

As seen in Figure 9, in going from one chromatogram to the next, the locations of the constituents (peaks 2 to 6) other than SO_2 (peak 1) shift to higher retention times in an ordered fashion. Calculations of the molecular weights have shown that in each chromatogram the incremental increase in molecular weight in going from peak 2 to 3 is 32 mass units, from peak 3 to 4 is equal to the the molecular weight of the respective olefin, from 4 to 5 is 32 mass units, and from 5 to 6 is 16 mass units. Based on the atomic weight of S being 32 and that of O being 16, some compositional possibilities were suggested for peaks 3 to 6. These have the form $[C_n^=][S]$ for peaks 3, $[C_n^=]_2[S]$ for peaks 4, $[C_n^=]_2[S][O]_2$ or $[C_n^=][S]_2$ for peaks 5, and $[C_n^=]_2[S][O]_3$ or $[C_n^=]_2[S]_2[O]$ for peaks 6, where $C_n^=$ represents C_4 olefin, C_5 olefin or C_6 olefin. Mechanisms for the formation of these structures were not advanced (18). Their formation probably involves some destruction of SO_2 in the presence of free radicals.

These polymers all show a two-step decomposition phenomenon (see Fig. 3). Selective trapping and analysis of the volatile decomposition products which form in the temperature range 100-200°C showed that only SO_2 and the respective olefin are formed in the first step of degradation.

In addition to these polyolefinsulfones, a sample of polystyrene-sulfone has been studied (1,8). SO_2 and styrene are found to be the major products of decomposition. Additional fragments derived from styrene dimers were observed as indicated by comparison of the results with those obtained from pyrolysis of polystyrenes; this provided evidence for the

presence of consecutive styrene residues in the repeat unit of the poly-styrenesulfone.
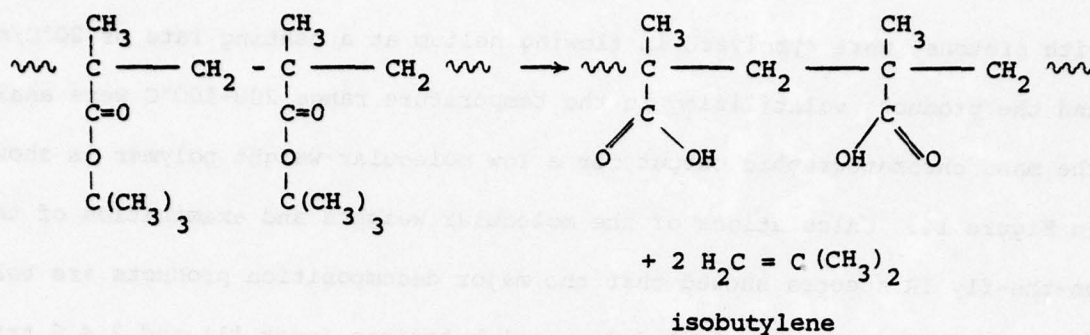
3) Polymethacrylates

Polymethylmethacrylates and polytertiarybutylmethacrylates of different tacticities have been studied by pyrolyzing samples in flowing helium atmosphere at a heating rate of 20°C/min (1).

Thermal conductivity responses during pyrolysis of polymethylmethacry-lates showed some differences for the different tactic forms (Figure 10). Analysis of the products of pyrolysis formed in the temperature range 200-500°C shows, however, that all the tactic forms revert almost exclusively to a single compound with a calculated molecular weight which compares well with that of the monomer, methylmethacrylate (Table I). Mass chromato-grams are shown in Figure 11. Analysis of the products of pyrolysis formed from the isotactic polymer in the temperature range 420-500°C (see Figure 10) has shown that in this region monomer formation is no longer observed (see Figure 11D). The traces of high molecular weight constituents ob-served were not characterized.

The thermal histories during pyrolysis of the polytertiarybutyl-methacrylates are shown in Figure 12. These polymers behave similarly and show two-stage decomposition. The mass chromatogram of the volatile products of pyrolysis formed in the temperature range 140-500°C is shown in Figure 13 for the isotactic polymer. The major products of decomposi-tion of all of the tactic forms are found to be isobutylene (peak 1) and the monomer, tertiarybutylmethacrylate (peak 2) (Table I). Formation of the monomer is a consequence of depolymerization. The formation of iso-butylene is indicative of ester decomposition, i.e.,

$$\sim\!\!\!\sim \underset{\underset{\underset{\underset{C(CH_3)_3}{|}}{O}}{|}}{\overset{\overset{\overset{CH_3}{|}}{C}}{|}}\!\!-\!\!CH_2\!-\!\underset{\underset{\underset{\underset{C(CH_3)_3}{|}}{O}}{|}}{\overset{\overset{\overset{CH_3}{|}}{C}}{|}}\!\!-\!\!CH_2 \sim\!\!\!\sim \longrightarrow \sim\!\!\!\sim \overset{\overset{\overset{CH_3}{|}}{C}}{|}\!\!-\!\!CH_2\!-\!\overset{\overset{\overset{CH_3}{|}}{C}}{|}\!\!-\!\!CH_2 \sim\!\!\!\sim$$

$$+\ 2\ H_2C = C\ (CH_3)_2$$

isobutylene

The relative extents of these reactions were found to be dependent on the tacticity of the sample as evidenced by differences in the monomer to iso-butylene peak height ratios measured in the outputs of the CO_2 channel of the mass chromatograph (1). Monomer to isobutylene ratio was found to be smallest for the syndiotactic and largest for the isotactic polymer. This observation was interpreted to mean that the extent of depolymerization compared with ester decomposition is greatest with the isotactic polymer; the steric hinderances of the bulky side groups apparently favor depolymer-ization most in the isotactic polymer. Further analyses of the volatile decomposition products formed in the temperature ranges 140 to 225°C, 140 to 320°C and 320 to 500°C in the isotactic polymer showed that all monomer generation takes place in the temperature range 140 to 320°C. In the second stage of decomposition (i.e., from 320 to 500°C) no monomer is generated, but some isobutylene continues to form.
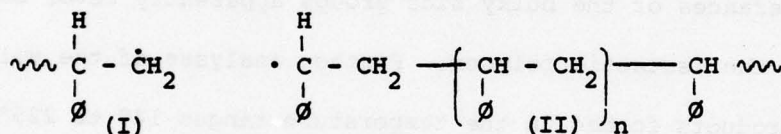
4) Polystyrenes

Anionic, thermal, and comb-shaped polystyrenes have been studied (3,9).

Anionic polystyrenes with different average molecular weights, which had been polymerized using n-butyl lithium as the initiator and terminated

with protons, were pyrolyzed in flowing helium at a heating rate of 20°C/min, and the products volatilizing in the temperature range 200-500°C were analyzed. The mass chromatographic output for a low molecular weight polymer is shown in Figure 14. Calculations of the molecular weights and examination of the on-the-fly IR spectra showed that the major decomposition products are toluene (peak 4), styrene (peak 5), 1,3-diphenyl-butadiene (peak 11) and 2,4,6 tri-phenyl-1-hexene (peak 16) (Table I and Table II). The relative amounts of these constituents have been found to depend on the molecular weight of the initial polymer. Among the constituents, toluene shows the highest sensitivity to molecular weight (Table II).

In polystyrene cleavage of the backbone results in the primary (I) and secondary (II) radicals.

$$\text{wv } \underset{\phi}{\overset{H}{C}} - \overset{\bullet}{C}H_2 \quad (I) \qquad \cdot \underset{\phi}{\overset{H}{C}} - CH_2 \left(\underset{\phi}{CH} - CH_2 \right)_n - \underset{\phi}{CH} \text{ wv } \quad (II)$$

Both of these can undergo depolymerization and form styrene (peak 5, Tables I and II).

1,3 diphenylbutadiene (peak 11, Tables I and II) forms from tertiary radicals of the form
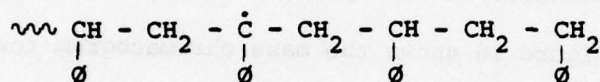
$$\text{wv } CH_2 - \overset{\bullet}{\underset{\phi}{C}} - CH_2 \text{ wv } ,$$
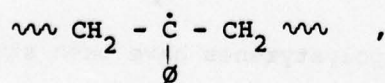
formed by hydrogen abstraction, which cleave β from the tertiary radical to form terminally unsaturated species with allylic hydrogens:

$$\text{---}CH_2 - \overset{\underset{\displaystyle \phi}{|}}{\overset{\displaystyle \bullet}{C}} - CH_2 - \overset{\underset{\displaystyle \phi}{|}}{CH}\text{---} \longrightarrow \text{---}CH_2 - \overset{\underset{\displaystyle \phi}{|}}{C} = CH_2 + \bullet\overset{\underset{\displaystyle \phi}{|}}{CH}\text{---}$$

Abstraction of the allylic hydrogen followed by β-scission of the resulting tertiary radical leads to 1,3 diphenylbutadiene:

$$\text{---}CH_2 - \overset{\underset{\displaystyle \phi}{|}}{CH} - \overset{\underset{\displaystyle \phi}{|}}{\overset{\displaystyle \bullet}{CH}} - \overset{\underset{\displaystyle \phi}{|}}{C} = CH_2 \longrightarrow \text{---}CH_2\bullet + CH = CH - \overset{\underset{\displaystyle \phi}{|}}{C} = CH_2$$
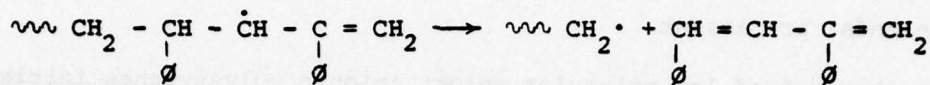
Intramolecular radical transfer in secondary radicals of type II, via a pseudo six-membered ring intermediate, may result in tertiary radicals such as:

$$\text{---}\overset{\underset{\displaystyle \phi}{|}}{CH} - CH_2 - \overset{\underset{\displaystyle \phi}{|}}{\overset{\displaystyle \bullet}{C}} - CH_2 - \overset{\underset{\displaystyle \phi}{|}}{CH} - CH_2 - CH_2$$

which upon β-scission to the left of the radical center leads to 2,4,6-triphenyl-1-hexene (peak 16, Tables I and II):

$$CH_2 = \overset{\underset{\displaystyle \phi}{|}}{C} - CH_2 - \overset{\underset{\displaystyle \phi}{|}}{CH} - CH_2 - CH_2$$
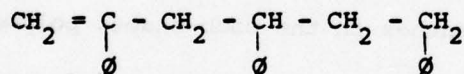
Depolymerization reactions in secondary radical II, if not stopped by other mechanisms, may eventually lead to the primary radical

$$\overset{\displaystyle \bullet}{\underset{\underset{\displaystyle \phi}{|}}{CH_2}}$$

which can abstract a hydrogen atom from another molecule to yield toluene (peak 4, Tables I and II).

Thermally polymerized polystyrenes have been found to display a different decomposition pattern from that of anionic polystyrenes. Comparison of the mass chromatograms shown in Figures 14 and 15 and examination of Table II shows that fewer products are formed with thermal polystyrenes; those peaks which are highly molecular weight dependent (i.e., influenced by chain ends) are absent.

Another set of low molecular weight anionic polystyrenes initiated with a di-carbanionic species and terminated at both ends with either proton, α-naphthyl, diphenylmethyl, or hydroxyl groups, was also studied. These polymers have been found to give products of decomposition which are similar to those of thermal polystyrenes. Polymers with α-naphthyl ends and diphenylmethyl ends showed some differences in that products arising from these groups are also observed. Figure 16 shows the mass chromatogram for the polymer with α-naphthyl ends. Peaks 5 and 6, predicted to be naphthylethane and 3-naphthyl-1-propene, respectively are characteristic of this polymer.

The major products of pyrolysis of comb-shaped polystyrenes were found to be similar to those of thermal polystyrenes also. However the steric hinderance of the side branches in the comb-shaped polymers was considered to affect the relative abundance of the observed constituents. Formation of the trimer (peak 16) is restricted and lesser amounts form.
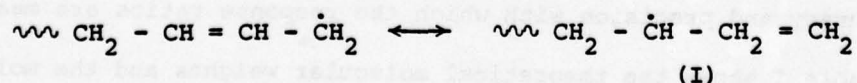
5) Polybutadienes

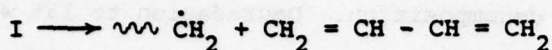1,4-polybutadienes with different cis/trans ratios have been studied (10).

Thermal histories before and during pyrolysis of a high trans and a high cis 1,4-polybutadiene in an inert atmosphere are shown in Figure 17. The polymers undergo two-step decomposition. Degradation to 15% weight loss and also after 15% weight loss has been investigated. Mass chromatograms of the volatile products formed during 15 weight percent degradation from a high cis and a high trans sample are shown in Figures 18 and 19, respectively. Calculation of the molecular weights and examination of on-the-fly IR spectra (Figure 20) have shown that the major products of decomposition are 1,3-butadiene (monomer, peak 1), cyclopentene (peak 2), 1,3-cyclohexadiene (peak 5) and 4-vinyl-1-cyclohexene (dimer , peak 9). Their relative amounts were found to vary with the cis/trans ratio in the polymer sample. The relative quantities of 4-vinyl-1-cyclohexene and 1,3-butadiene decrease, cyclopentene increases and 1,3-cyclohexadiene is relatively unchanged with increasing trans content as shown in Figure 21.

The mass chromatogram of the products of pyrolysis after 15 percent weight loss of high trans 1,4-polybutadiene (Figure 22) showed that 4-vinyl-1-cyclohexene, which is the most abundant product in degradation to 15% weight loss (see Figure 19), is only a minor product of further decomposition.
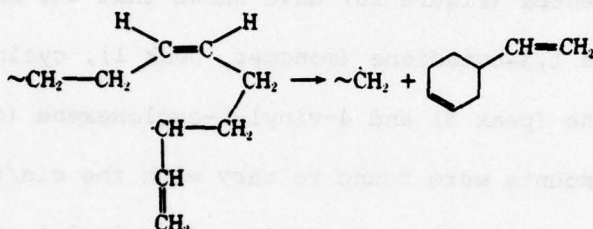
The major products of decomposition of polybutadienes are accounted for by a free radical mechanism. Homolytic scission of the single bond of the polymer chain at a site which is β to the double bond results in the radical

$$\sim\!\!\sim CH_2 - CH = CH - \dot{C}H_2 \longleftrightarrow \sim\!\!\sim CH_2 - \dot{C}H - CH_2 = CH_2$$

(I)

The monomer 1,3-butadiene arises from I via β-scission, i.e.,

$$I \longrightarrow \sim\!\!\sim\!\!\sim \dot{C}H_2 + CH_2 = CH - CH = CH_2$$

4-vinyl-1-cyclohexene arises via a backbiting step involving a pseudo
six-membered ring intermediate which is favored by a cis 1,4-structure,
as is indicated by

1,2-vinyl-polybutadiene has also been studied (10). In contrast
to 1,4-polybutadienes, this polymer undergoes one-step decomposition.
The mass chromatogram of all of the volatile products of pyrolysis was
similar to that from pyrolysis above 15% weight loss for 1,4-polybutadienes
(compare Fig. 4 and Fig. 22). This observation has been interpreted to
suggest that part of the 1,4-structure undergoes isomerization to the
1,2-structure in the course of being heated to 15% weight loss.

COMMENTS ON CALCULATED MASS NUMBERS

The accuracy of the molecular weight determination using a mass
chromatograph depends on the invariance of the instrument constant and
the accuracy and precision with which the response ratios are measured (11).

Table I shows the theoretical molecular weights and the molecular
weights calculated from the mass chromatographic outputs for some of the

assigned structures in the pyrograms discussed in the foregoing sections. As seen from this table, the calculated values are acceptable values, and thus the mass chromatograph offers a convenience not found in the usual gas chromatograph-mass spectrometer combinations. Mass spectrometry, even though more accurate, requires elaborate interfacial systems and sophisti-cated data-reduction processes.

CONCLUDING REMARKS

The results presented in the foregoing sections show the utility and power of the on-line pyrolysis system in polymer analysis. The system provides thermal history before and during pyrolysis and makes selective trapping and analysis of volatile constituents possible. Chromatographic retention times, easily calculable mass numbers, computer-added IR spectra -- all available from an on-line system -- facilitate identification of the volatile constituents. Thus not only are fingerprint pyrograms generated, but also detailed information about the products of pyrolysis and their relative abundances are obtained. Based on these, mechanisms for decompo-sition become easier to propose and to verify.

REFERENCES

1. E. Kiran, Ph.D. Thesis, Department of Chemical Engineering, Princeton University, Princeton, N. J. (1974).

2. E. Kiran and J. K. Gillham, J. Appl. Polym. Sci., 20, 931 (1976).

3. H. H. Kuo, Ph.D. Thesis, Department of Chemical Engineering, Princeton University, Princeton, N. J. (1976).

4. E. Kiran and J. K. Gillham, ACS, Polymer Preprints, 14(1), 580 (1973).

5. E. Kiran and J. K. Gillham, Soc. Plastics Engineers, Tech. Papers, 19, 502 (1973).

6. E. Kiran and J. K. Gillham, J. Macromol. Sci.-Chem. A8(1), 211 (1974).

7. E. Kiran and J. K. Gillham, J. Appl. Poly. Sci., 20, 2045 (1976).

8. E. Kiran, J. K. Gillham and E. Gipstein, J. Appl. Poly. Sci., 21, 1159 (1977).

9. H. H. Kuo, H. A. Pffeffer and J. K. Gillham, Amer. Chem. Soc., Coatings and Plastics Preprints, 35(1), 434 (1975).

10. S. Tamura and J. K. Gillham, J. Appl. Poly. Sci., 22, 1867 (1978).

11. E. Kiran and J. K. Gillham, Anal. Chem. 47(7), 983 (1975).

12. S. S. Stivala and S. M. Gabbay, in "Aspects of Degradation and Stabilization of Polymers", H. H. G. Jellinek (ed.), Elsevier, New York, 1978, Chapter 13.

13. T. L. Cottrell, "The Strength of Chemical Bonds", Butterworth, London, 1958.

ACKNOWLEDGMENT

TABLE I. Calculated Molecular Weights and Assigned Structures
for some of the Characteristic Peaks in the Pyrograms
discussed in this paper.

Figure No	Peak No	Assigned Structure	Molecular Weight	
			Theory	Calculated
6	6	Hexene	84	85.1
	6'	Hexane	86	85.5
	10	Decene	140	141.6
	10'	Decane	142	142.9
	14	Tetradecene	196	195.4
	20	Eicosene +(eicosane)	(283)	287.4
7	3	pentane	72	77
	5	2 methylpentane	86	86
	9	2,4 dimethyl-1-heptene	126	124.7
	11	2,4,6 trimethylnonane	170	171
	12	2,4,6,8 tetramethyl-1-hendecene	210	210.7
	16	2,4,6,8,10,12 hexamethyl-1-tridecene	266	270.4
8	6	2,2,4 trimethylpentane	114	112.2
	12	2,4,4,6,6 pentamethyl-1-heptene	168	170.5
	16	2,4,4,6,6,8,8 heptamethyl-1-nonene	224	227
	20	2,4,4,6,6,8,8,10,10 nonamethyl-1-hendecene	280	277.2
	24	2,4,4,6,6,8,8,10,10,12,12 undecamethyl-1-tridecene	336	325
11	1	methylmethacrylate	100	100.3
13	1	isobutylene	56	60.1
	2	tertiarybutylmethacrylate	142	136
14,15	4	toluene	92	93
	5	styrene	104	109
	11	1,3 diphenylbutadiene	206	205
	16	2,4,6 triphenyl-1-hexene	313	339
18,19	1	1,3 butadiene	54	56.3
	2	cyclopentene	68	68.7
	5	1,3-cyclohexadiene	80	77.2
	9	4-vinyl-1-cyclohexene	108	108.8

TABLE II. Volatile Products of Pyrolysis of Anionic and Thermal Polystyrenes. Variation of their Relative Amounts (as weight percentages) with the Molecular Weight of the Initial Polymer.

Peak/$\overline{Mn}$ Number	Anionic					Thermal		
	2100	4000	10,000.	20,400	390,000	1880	6270	111,000
1	.076	.031	Trace	Trace	0	0	0	0
2	.69	.37	Trace	Trace	0	0	0	0
3	.71	.38	1.77	2.97	1.82	0	0.32	0
4	8.33	5.24	2.79	1.99	1.31	1.0	1.40	2.54
5	37.4	35.8	41.2	45.7	49.0	42.80	48.00	50.90
6	4.14	1.61	Trace	Trace	0	0	0	0
7	2.72	3.64	Trace	Trace	0	0	0	0
8	2.56	1.14	Trace	Trace	0	0	0	0
9	3.02	2.75	3.39	3.04	2.22	0	0	0
10	4.11	5.25	5.75	4.36	5.91	Trace	Trace	Trace
11	8.96	9.76	12.56	11.74	11.37	17.50	18.00	18.87
12	1.66	1.17	.50	Trace	0	0	0	0
13	2.99	2.23	1.27	Trace	0	0	0	0
14	4.53	5.85	6.45	7.19	5.07	0	0	0
15	5.75	7.63	7.38	6.57	8.69	0	0	0
16	22.33	18.14	16.70	16.44	14.64	35.60	29.80	26.33

FIGURE CAPTIONS

Figure 1. Schematic diagram of the laboratory for pyrolytic studies.

Figure 2. Coupling of the pyrolyzer with the thermal conductivity detector, the trap, and the mass chromatograph.

Figure 3. Left: Thermal history before and during pyrolysis of poly(pentene-1-sulfone) ($[\eta] = 1.49$ dℓ/g).

Right: Mass chromatogram of the volatile pyrolysis products of poly(pentene-1-sulfone). Peak attenuations were X256 for peaks 1 and 2, and X16 thereafter. The columns (SE-30) were program-heated at 5°C/min from 30° to 300°C.

Figure 4. Mass chromatogram of the volatile pyrolysis products of syndiotactic 1,2-polybutadiene (1,2 structure 83-90%, $\overline{M}_w = 177,000$, $\overline{M}_n = 107,000$) formed during 100% weight loss. Peak attenuations for the Freon-115 channel were X64 for peak 1, and X16 thereafter. Those for the CO_2 channel were X8 for all peaks. The columns (Dexsil 300) were program-heated at 4°C/min from 30° to 300°C. The broad peak at the extreme left shows the thermal conductivity cell response during pyrolysis; the subsequent sharp peak shows the response during flash release of the products from the pyrolyzer trap.

Figure 5. Schematic of the coupling of the gas chromatograph with the fast scan vapor-phase infrared spectrophotometer and the computer.

Figure 6. Mass chromatogram of the volatile pyrolysis products of low density polyethylene ($\overline{M}_w$ = 140,000, $\overline{M}_n$ = 16,000). Peak attenuations were X8, except for peaks 3 and 4 in the Freon-115 channel for which the attenuations were X64. Columns (SE-30) were program-heated at 5°C/min from 30-300°C.

Figure 7. Mass chromatogram of the volatile pyrolysis products of isotactic poly-propylene ($\sim$100% isotactic, $\overline{M}_w$ = 284,000 and $\overline{M}_w/\overline{M}_n$ = 2.98). In the CO_2 channel peak attenuations were X32 for peak 9, and X8 for all others. In the Freon-115 channel attenuations were X128 (Peak 1), X64 (peaks 2 through 5), X32 (peaks 6 through 11), and X8 thereafter. Columns (SE-30) were program-heated at 7°C/min from 30° to 300°C.

Figure 8. Mass chromatogram of the volatile pyrolysis products of polyisobutylene ($\overline{M}_V$ = 120,000). Peak attenuations were X8 in both channels, except for peaks 1 and 2 for which the setting was X128. Columns (SE-30) were program-heated at 5°C/min from 30° to 300°C.

Figure 9. Comparison of the CO_2 channels of the mass chromatograms of volatile pyrolysis products of poly(butene-1-sulfone) (top), poly(pentene-1-sulfone) (middle), and poly(hexene-1-sulfone) (bottom).

Figure 10. Thermal conductivity cell responses during pyrolysis of atactic ($\overline{M}_w$ = 105,000, $\overline{M}_w/\overline{M}_n$ = 2.15), syndiotactic (70% syndio, $\overline{M}_w$ = 83200, $\overline{M}_w/\overline{M}_n$ = 1.33) and isotactic (91.5% iso, $\overline{M}_w$ = 2,780,500 $\overline{M}_w/\overline{M}_n$ = 2.28) polymethylmethacrylates.

Figure 11. Mass chromatogram of the volatile products of pyrolysis formed in the

temperature range 200-500°C of atactic (A), syndiotactic (B)

and isotactic (C) polymethylmethacrylates. Only the CO_2 channel

outputs are shown for the syndiotactic and isotactic polymers. Columns

(Dexsil-300) were program-heated at 5°C/min from 30 to 300°C.

Peak attenuations were X64 for peak 1, and X8 for all others.

The figure at the bottom (D) shows the CO_2 channel output for

the products formed from the isotactic polymer in the tempera-

ture range 420 to 500°C.

Figure 12. Thermal conductivity cell responses during pyrolysis of atactic

($\overline{M}_w$ = 359,950, $\overline{M}_w/\overline{M}_n$ = 2.03), syndiotactic ($\overline{M}_w$ = 20940, $\overline{M}_w/\overline{M}_n$ =

1.49) and isotactic (82% iso, $\overline{M}_w$ = 300,000, $\overline{M}_w/\overline{M}_n$ = 1.13)

poly(tertiarybutylmethacrylate)s.

Figure 13. Mass chromatogram of the volatile products of pyrolysis of isotactic

poly(tertiarybutylmethacrylate). Columns (Dexsil-300) were

program-heated at 5°C/min from 30° to 300°C. Peak attenuations

were X8, except for peak 1 for which the settings were X128

in the Freon channel and X16 in the CO_2 channel.

Figure 14. Mass chromatogram of the volatile products of pyrolysis of anionic

polystyrene ($\overline{M}_n$ = 2100, $\overline{M}_w/\overline{M}_n$ < 1.1) with n-butyl ends. Columns

(Dexil-300) were program-heated at 5°C/min from 30° to 300°C.

Figure 15. Mass chromatogram of the volatile products of pyrolysis of thermal poly-

styrene ($\overline{M}_n$ = 1880, $\overline{M}_w/\overline{M}_n$ = 1.01). Columns (Dexsil 300)

were program-heated at 5°C/min from 30° to 300°C.

Figure 16. Mass chromatogram of the volatile products of pyrolysis of anionic

polystyrene ($\overline{M}_n$ = 10500, $\overline{M}_w/\overline{M}_n$ = 1.15) with α-naphthyl ends.

Columns (Dexsil-300) were program-heated at 5°C/min from 30°

to 300°C.

Figure 17. Thermal history before and during pyrolysis of 1,4-polybutadienes.

Solid lines for sample with 87% trans, $\overline{M}_w$ = 67300, $\overline{M}_w/\overline{M}_n$ = 2.18;

and dashed lines for sample with 0% trans, $\overline{M}_w$ = 633,500, $\overline{M}_w/\overline{M}_n$ =

3.62.

Figure 18. Mass chromatogram of the volatile pyrolysis products of high cis 1,4-poly-

butadiene (0% trans, $\overline{M}_w$ = 633,500, $\overline{M}_w/\overline{M}_n$ = 3.62) formed during

15 percent weight loss.   Columns (Dexsil-300) were

program-heated at 4°C/min from 30° to 300°C. Peak attenuations

for the Freon-115 channel were X64 for peak 1, and X16 thereafter.
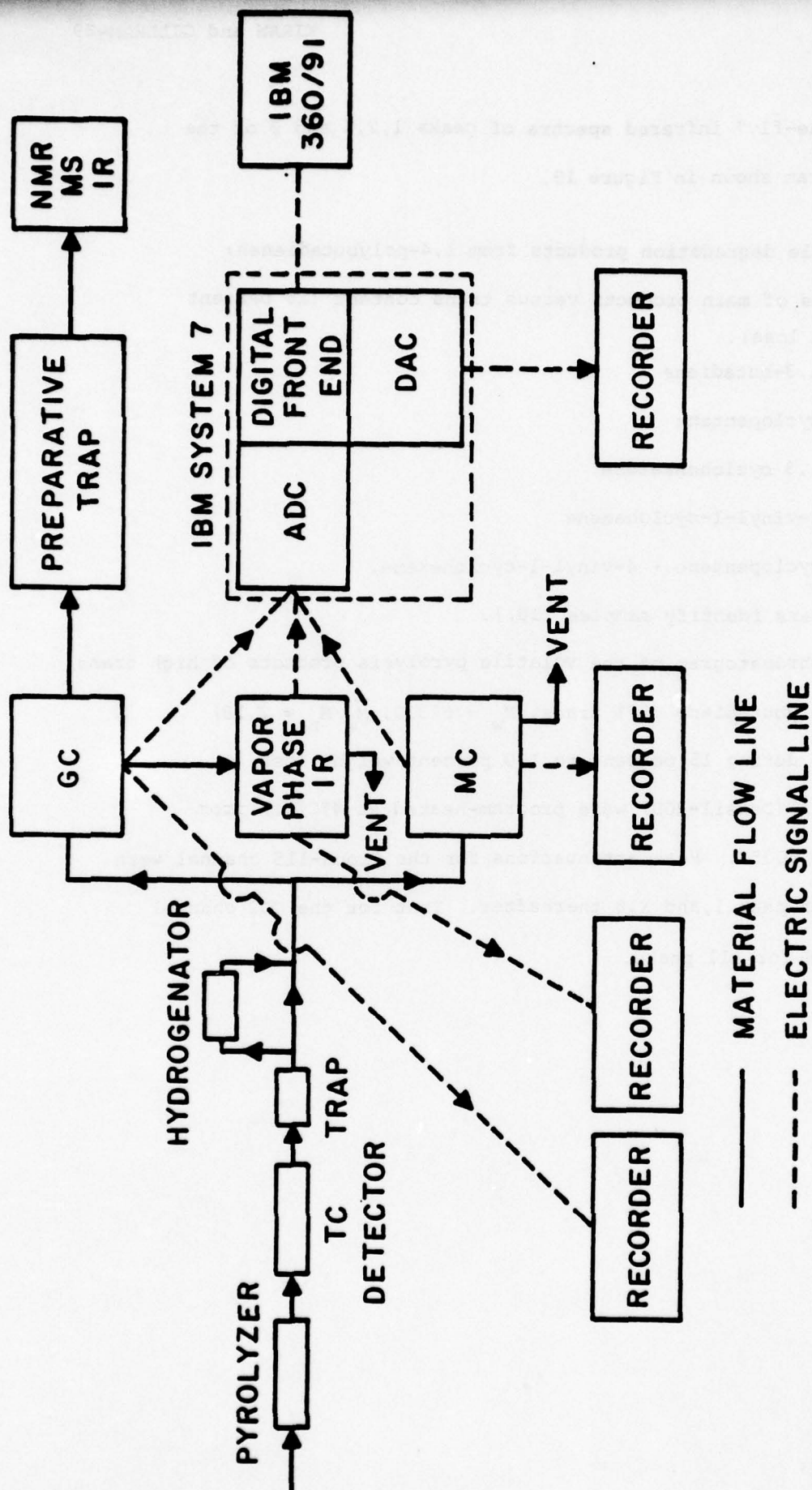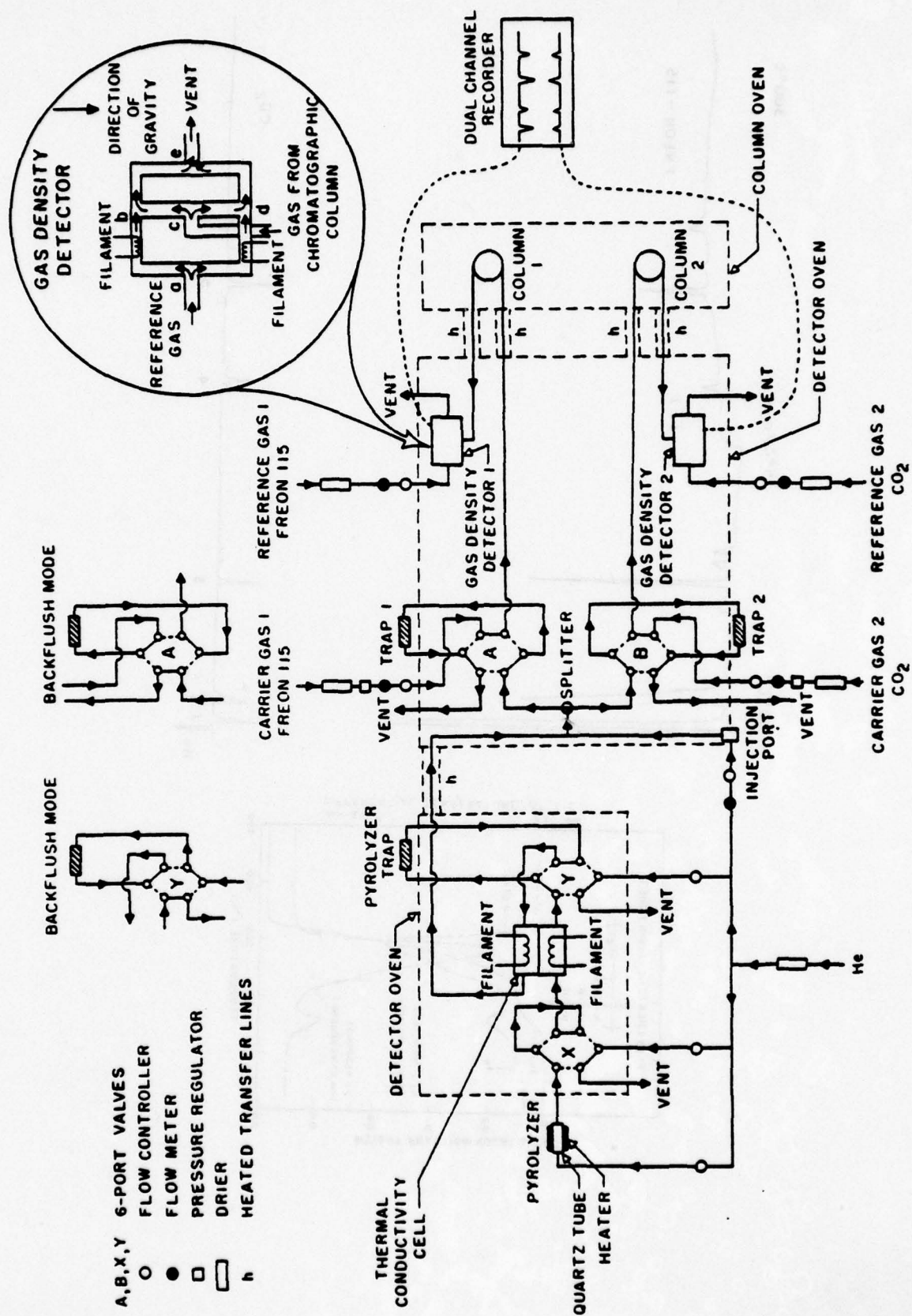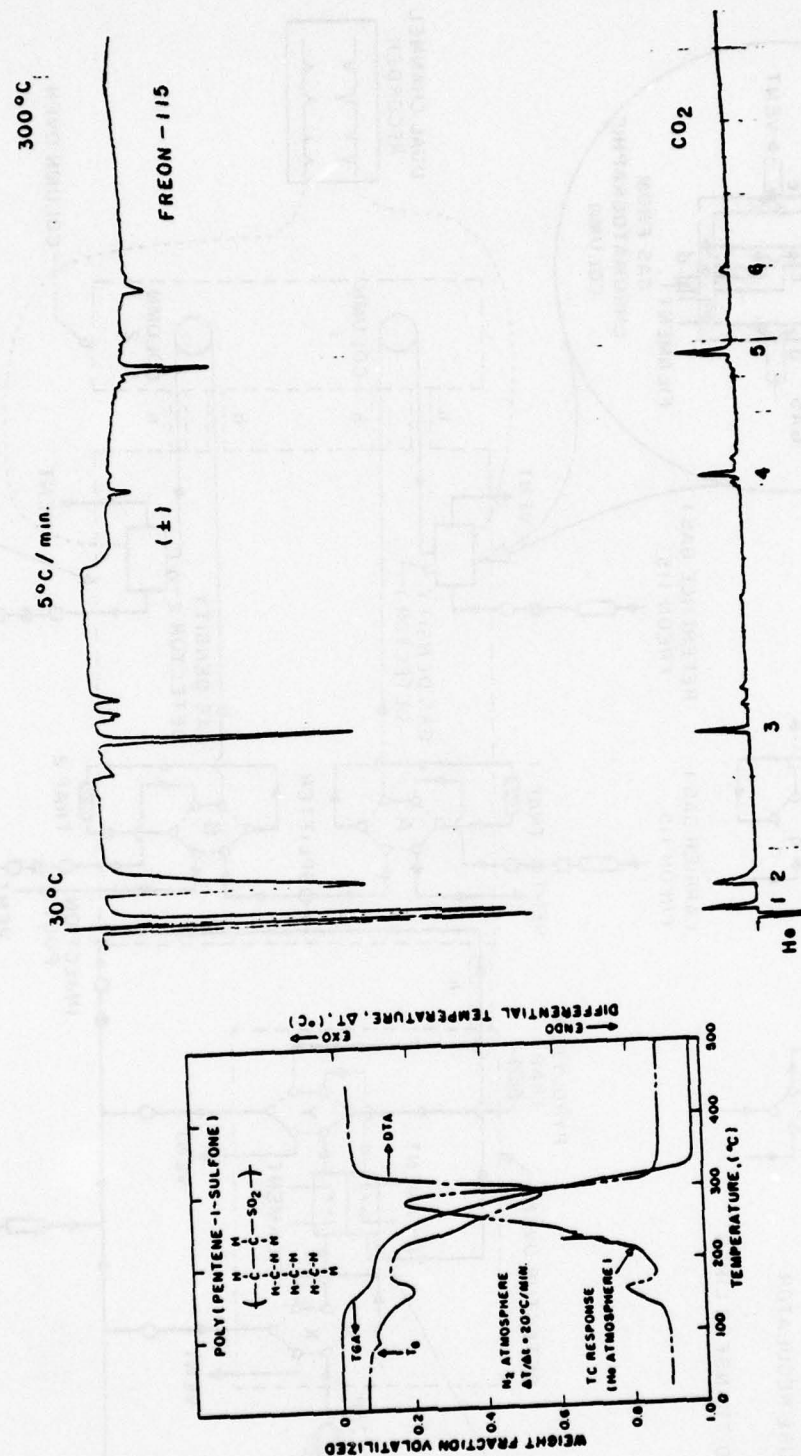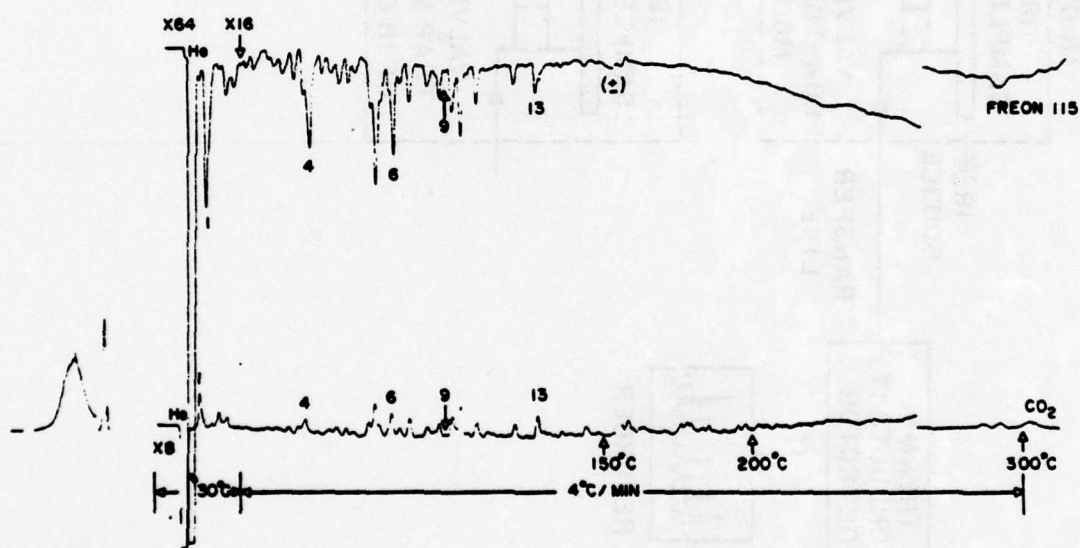
That for the CO_2 channel was X8 for all peaks.

Figure 19. Mass chromatogram of the volatile pyrolysis products of high trans 1,4-

polybutadiene (87% trans, $\overline{M}_w$ = 67300, $\overline{M}_w/\overline{M}_n$ = 2.18) formed during

15 percent weight   loss.   Columns (Dexsil-300) were program-

heated at 4°C/min from 30° to 300°C. Peak attenuations for the

Freon-115 channel were X64 for peak 1, and X16 thereafter. That

for the CO_2 channel was X8 for all peaks.

Figure 20. "On-the-fly" infrared spectra of peaks 1,2,5 and 9 of the

pyrogram shown in Figure 19.

Figure 21. Volatile degradation products from 1,4-polybutadienes:

amounts of main products versus trans content (15 percent

weight loss).

● 1,3-butadiene

◑ cyclopentene

◑ 1,3 cyclohexadiene

○ 4-vinyl-1-cyclohexene

△ cyclopentene + 4-vinyl-1-cyclohexene.

[Numbers identify samples (10)].

Figure 22. Mass chromatogram of the volatile pyrolysis products of high trans

1,4-polybutadiene (87% trans, $\overline{M}_w$ = 67300, $\overline{M}_w/\overline{M}_n$ = 2.18)

formed during 15 percent to 100 percent weight loss.

Columns (Dexsil-300) were program-heated at 4°C/min from

30° to 300°C. Peak attenuations for the Freon-115 channel were

X64 for peak 1,and X16 thereafter. That for the CO_2 channel

was X8 for all peaks.

Fig. 1

MATERIAL FLOW LINE
ELECTRIC SIGNAL LINE

Figure 2

Figure 3

FREON – 115

300°C

5°C / min.

(±)

30°C

He

CO₂

1 2   3   4   5   6

DIFFERENTIAL TEMPERATURE, ΔT, (°C)
ENDO → | ← EXO

POLY (PENTENE-1-SULFONE)

$$\begin{array}{c} H-C-H \\ H-C-H \\ H-C-H \\ H \end{array}$$

N₂ ATMOSPHERE
ΔT/Δt = 20°C/MIN.

TC RESPONSE
(He ATMOSPHERE)

DTA

TGA

T₀

WEIGHT FRACTION VOLATILIZED

0

0.2

0.4

0.6

0.8

1.0

TEMPERATURE, (°C)

100   200   300   400   500

Figure 4

Fig. 5

Fig. 6

30°C   7°C/MIN.   300°C

(±)   FREON-115

He   2 3 4 5   6 7 8   9   10 11   12 13   14 15   16 17 18 19   20 21 22 CO_2

Fig. 7

Fig. 8

Fig. 9

POLY (METHYL METHACRYLATE) S

HELIUM ATMOSPHERE
$\Delta T / \Delta t = 20°C / MIN.$

ATACTIC

SYNDIOTACTIC

ISOTACTIC

THERMAL CONDUCTIVITY CELL RESPONSE

TEMPERATURE, (°C)

Fig. 10

Freon-115

(A) atactic PMMA

CO_2

He   1

(B) syndiotactic PMMA CO_2

He   1

(C) isotactic PMMA CO_2

He

(D) isotactic PMMA CO_2

He

Fig. 11

POLY(t-BUTYL METHACRYLATE)S

ATACTIC

HELIUM ATMOSPHERE
ΔT/Δt = 20°C/MIN.

SYNDIOTACTIC

ISOTACTIC

THERMAL CONDUCTIVITY CELL RESPONSE
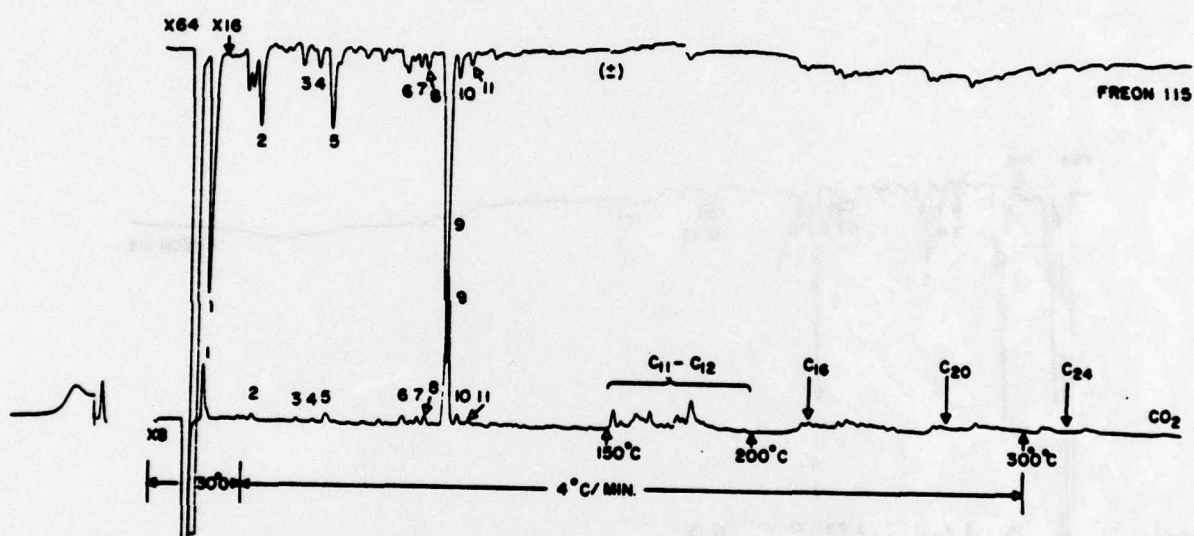
TEMPERATURE, (°C)

Fig. 12

Fig. 13

Fig. 14

Fig. 15
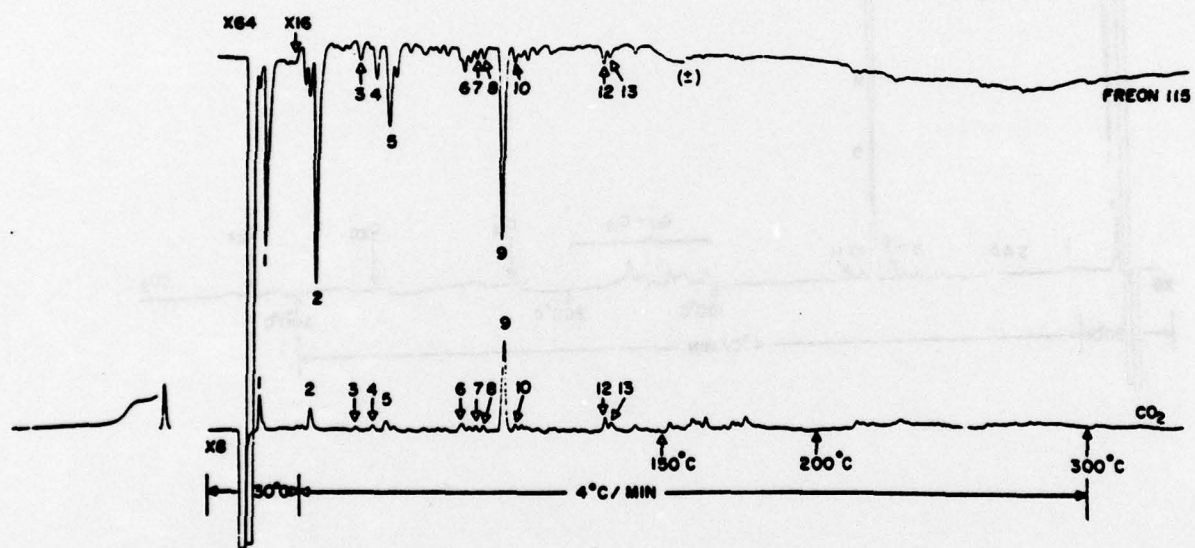
Fig. 16
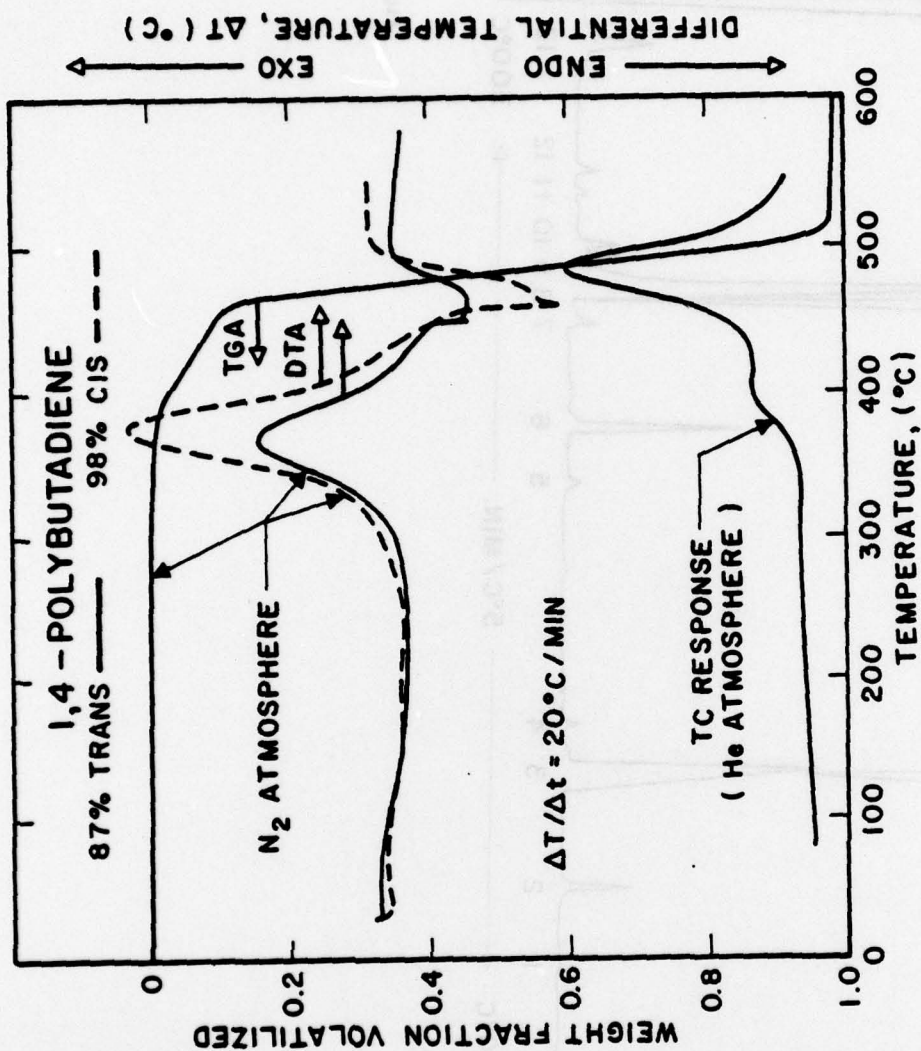
Figure 17

Figure 18

Figure 19
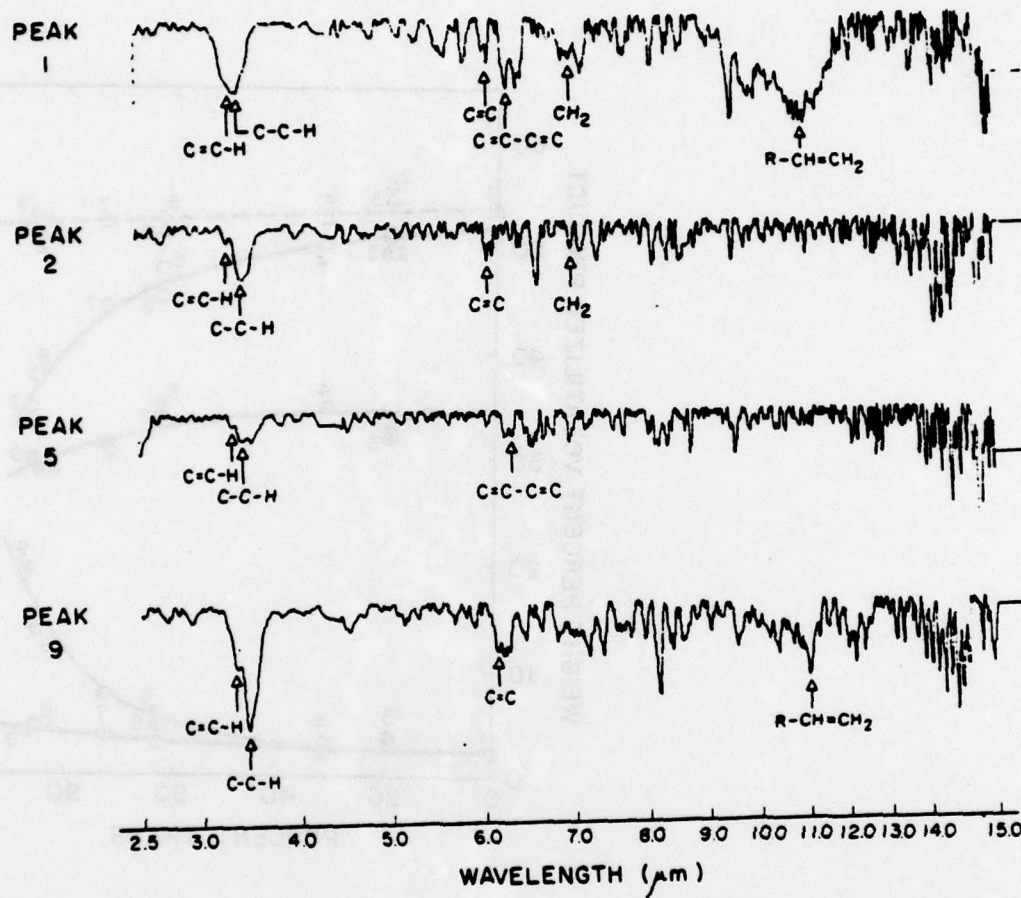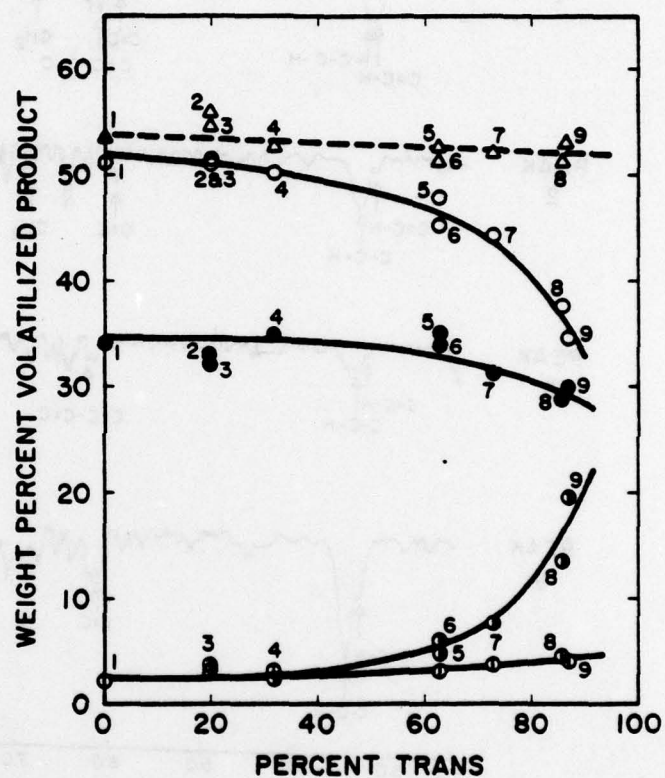
Figure 20

Figure 21
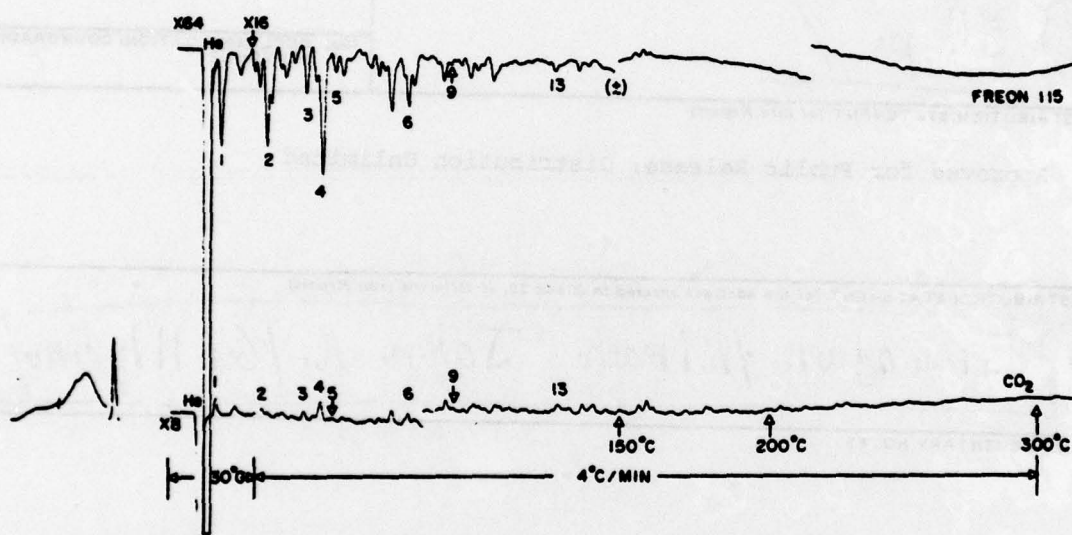
Figure 22

REPORT DOCUMENTATION PAGE

READ INSTRUCTIONS BEFORE COMPLETING FORM

1. REPORT NUMBER	2. GOVT ACCESSION NO.	3. RECIPIENT'S CATALOG NUMBER
Technical Report No. 16	TR-16	

4. TITLE (and Subtitle)
Pyrolysis-Molecular Weight Chromatography-Vapor Phase Infrared Spectrophotometry: An On-Line System for Analysis of Polymers

5. TYPE OF REPORT & PERIOD COVERED
Technical Report, April 1978-April 1979

6. PERFORMING ORG. REPORT NUMBER

7. AUTHOR(s)
E. Kiran and J. K. Gillham

8. CONTRACT OR GRANT NUMBER(s)
N00014-76-C-0200

9. PERFORMING ORGANIZATION NAME AND ADDRESS
Polymer Materials Program
Department of Chemical Engineering
Princeton University, Princeton, NJ 08544

10. PROGRAM ELEMENT, PROJECT, TASK AREA & WORK UNIT NUMBERS
Task No. NR 356-504

11. CONTROLLING OFFICE NAME AND ADDRESS
Office of Naval Research
800 North Quincy St.
Arlington, VA 22217

12. REPORT DATE
May 1979

13. NUMBER OF PAGES
51

14. MONITORING AGENCY NAME & ADDRESS(If different from Controlling Office)
57 p.

15. SECURITY CLASS. (of this report)

15a. DECLASSIFICATION/DOWNGRADING SCHEDULE

16. DISTRIBUTION STATEMENT (of this Report)

Approved for Public Release; Distribution Unlimited

17. DISTRIBUTION STATEMENT (of the abstract entered in Block 20, if different from Report)

Erdogan/Kiran John K./Gillham

18. SUPPLEMENTARY NOTES

19. KEY WORDS (Continue on reverse side if necessary and identify by block number)

Pyrolysis
Mass Chromatography
Vapor Phase Infrared Spectrophotometry
Polyolefins

Poly olefin sulfones
Poly methacrylates
Polystyrenes
Polybutadienes

20. ABSTRACT (Continue on reverse side if necessary and identify by block number)

An on-line pyrolysis system has been developed which comprises a programmable pyrolyzer, a thermal conductivity cell, a trap, a mass chromatograph, a conventional gas chromatograph, a vapor-phase infrared spectrophotometer, and a digital computer. The system has proved powerful for analysis of polymers as has been shown by results obtained with polyolefins, polyolefinsulfones, polymethacrylates, polystyrenes and polybutadienes. This report provides a brief description of the system and reviews results obtained with these polymers.

DD FORM 1473 **1 JAN 73**   EDITION OF 1 NOV 65 IS OBSOLETE
S/N 0102-LF-014-6601

402 377

TECHNICAL REPORT DISTRIBUTION LIST, GEN

	No. Copies		No. Copies
Office of Naval Research 800 North Quincy Street Arlington, Virginia 22217 Attn: Code 472	2	Defense Documentation Center Building 5, Cameron Station Alexandria, Virginia 22314	12
ONR Branch Office 536 S. Clark Street Chicago, Illinois 60605 Attn: Dr. George Sandoz	1	U.S. Army Research Office P.O. Box 1211 Research Triangle Park, N.C. 27709 Attn: CRD-AA-IP	1
ONR Branch Office 715 Broadway New York, New York 10003 Attn: Scientific Dept.	1	Naval Ocean Systems Center San Diego, California 92152 Attn: Mr. Joe McCartney	1
ONR Branch Office 1030 East Green Street Pasadena, California 91106 Attn: Dr. R. J. Marcus	1	Naval Weapons Center China Lake, California 93555 Attn: Dr. A. B. Amster Chemistry Division	1
ONR Area Office One Hallidie Plaza, Suite 601 San Francisco, California 94102 Attn: Dr. P. A. Miller	1	Naval Civil Engineering Laboratory Port Hueneme, California 93401 Attn: Dr. R. W. Drisko	1
ONR Branch Office Building 114, Section D 666 Summer Street Boston, Massachusetts 02210 Attn: Dr. L. H. Peebles	1	Professor K. E. Woehler Department of Physics & Chemistry Naval Postgraduate School Monterey, California 93940	1
Director, Naval Research Laboratory Washington, D.C. 20390 Attn: Code 6100	1	Dr. A. L. Slafkosky Scientific Advisor Commandant of the Marine Corps (Code RD-1) Washington, D.C. 20380	1
The Assistant Secretary of the Navy (R,E&S) Department of the Navy Room 4E736, Pentagon Washington, D.C. 20350	1	Office of Naval Research 800 N. Quincy Street Arlington, Virginia 22217 Attn: Dr. Richard S. Miller	1
Commander, Naval Air Systems Command Department of the Navy Washington, D.C. 20360 Attn: Code 310C (H. Rosenwasser)	1	Naval Ship Research and Development Center Annapolis, Maryland 21401 Attn: Dr. G. Bosmajian Applied Chemistry Division	1
		Naval Ocean Systems Center San Diego, California 91232 Attn: Dr. S. Yamamoto, Marine Sciences Division	1

Encl 1

TECHNICAL REPORT DISTRIBUTION LIST, 356A

	No. Copies		No. Copies

Dr. Stephen H. Carr
Department of Materials Science
Northwestern University
Evanston, Illinois 60201 — 1

Dr. M. Broadhurst
Bulk Properties Section
National Bureau of Standards
U.S. Department of Commerce
Washington, D.C. 20234 — 2

Dr. T. A. Litovitz
Department of Physics
Catholic University of America
Washington, D.C. 20017 — 1

Dr. R. V. Subramanian
Washington State University
Department of Materials Science
Pullman, Washington 99163 — 1

Dr. M. Shen
Department of Chemical Engineering
University of California
Berkeley, California 94720 — 1

Dr. V. Stannett
Department of Chemical Engineering
North Carolina State University
Raleigh, North Carolina 27607 — 1

Dr. D. R. Uhlmann
Department of Metallurgy and Material
   Science
Center for Materials Science and
   Engineering
Massachusetts Institute of Technology
Cambridge, Massachusetts 02139 — 1

Naval Surface Weapons Center
White Oak
Silver Spring, Maryland 20910
Attn: Dr. J. M. Augl
      Dr. B. Hartman — 1

Dr. G. Goodman
Globe Union Incorporated
5757 North Green Bay Avenue
Milwaukee, Wisconsin 53201 — 1

Picatinny Arsenal
SMUPA-FR-M-D
Dover, New Jersey 07801
Attn: A. M. Anzalone
      Building 3401 — 1

Dr. J. K. Gillham
Princeton University
Department of Chemistry
Princeton, New Jersey 08540 — 1

Douglas Aircraft Co.
3855 Lakewood Boulevard
Long Beach, California 90846
Attn: Technical Library
      Cl 290/36-84
      AUTO-Sutton — 1

Dr. E. Baer
Department of Macromolecular Science
Case Western Reserve University
Cleveland, Ohio 44106 — 1

Dr. K. D. Pae
Department of Mechanics and
   Materials Science
Rutgers University
New Brunswick, New Jersey 08903 — 1

NASA-Lewis Research Center
21000 Brookpark Road
Cleveland, Ohio 44135
Attn: Dr. T. T. Serofini, MS-49-1 — 1

Dr. Charles H. Sherman, Code TD 121
Naval Underwater Systems Center
New London, Connecticut — 1

Dr. William Risen
Department of Chemistry
Brown University
Providence, Rhode Island 02192 — 1

Dr. Alan Gent
Department of Physics
University of Akron
Akron, Ohio 44304 — 1

TECHNICAL REPORT DISTRIBUTION LIST, 356A

	No. Copies		No. Copies

Mr. Robert W. Jones
Advanced Projects Manager
Hughes Aircraft Company
Mail Station D 132
Culver City, California 90230   1

Dr. C. Giori
IIT Research Institute
10 West 35 Street
Chicago, Illinois 60616   1

Dr. M. Litt
Department of Macromolecular Science
Case Western Reserve University
Cleveland, Ohio 44106   1

Dr. R. S. Roe
Department of of Materials Science
  and Metallurgical Engineering
University of Cincinnati
Cincinnati, Ohio 45221   1

Dr. L. E. Smith
U.S. Department of Commerce
National Bureau of Standards
Stability and Standards
Washington, D.C. 20234   1

Dr. Robert E. Cohen
Chemical Engineering Department
Massachusetts Institute of Technology
Cambridge, Massachusetts 02139   1

Dr. David Roylance
Department of Materials Science and
  Engineering
Massachusetts Institute of Technology
Cambridge, Massachusetts 02039   1

Dr. T. P. Conlon, Jr., Code 3622
Sandia Laboratories
Sandia Corporation
Albuquerque, New Mexico   1

Dr. Martin Kaufmann, Head
Materials Research Branch, Code 4542
Naval Weapons Center
China Lake, California 93555   1

Dr. T. J. Reinhart, Jr., Chief   1
Composite and Fibrous Materials Branch
Nonmetallic Materials Division
Department of the Air Force
Air Force Materials Laboratory (AFSC)
Wright-Patterson Air Force Base, Ohio 45432

Dr. J. Lando
Department of Macromolecular Science
Case Western Reserve University   1
Cleveland, Ohio 44106

Dr. J. White
Chemical and Metallurgical Engineering
University of Tennessee
Knoxville, Tennessee 37916   1

Dr. J. A. Manson
Materials Research Center
Lehigh University
Bethlehem, Pennsylvania 18015   1

Dr. R. F. Helmreich
Contract RD&E
Dow Chemical Co.
Midland, Michigan 48640   1

Dr. R. S. Porter
University of Massachusetts
Department of Polymer Science and
  Engineering
Amherst, Massachusetts 01002   1

Professor Garth Wilkes
Department of Chemical Engineering
Virginia Polytechnic Institute and
  State University
Blacksburg, Virginia 24061   1

Dr. Kurt Baum
Fluorochem Inc.
6233 North Irwindale Avenue
Azuza, California 91702   1

Professor C. S. Paik Sung
Department of Materials Sciences and
  Engineering
Massachusetts Institute of Technology
Cambridge, Massachusetts 02139   1

2